Characterization of food stuffs using magnetic resonance elastography

Gruwel, Marco L. H.; Latta, Peter; Matwiy, Brendon; Tomanek, Boguslaw

Publisher's version / Version de l'éditeur:
https://doi.org/10.1016/j.foodres.2010.07.015
Food Research International, 43, 8, pp. 2087-2092, 2010-10-01

Characterization of food stuffs using Magnetic Resonance Elastography

Marco L.H. Gruwel[a,*], Peter Latta[a,b], Brendon Matwiy[a], Boguslaw Tomanek[a]

[a]*NRC-CNRC Institute for Biodiagnostics, 435 Ellice Avenue, Winnipeg MB, R3B 1Y6 Canada*
[b]*Slovak Academy of Sciences, Institute for Measurement Science, Dúbravská cesta 9, SK-84219 Bratislava, Slovakia*

Abstract

Viscoelastic properties of formulated food products are often associated with the textural properties of the material. Plasticity provides an important food quality factor. Unfortunately, viscoelastic properties of food stuffs are normally measured in the bulk phase, prior to packaging. Here we describe the application of a Magnetic Resonance Elastography (MRE) method using a specially designed sample holder for fast, reproducible and non-invasive measurement of spatially averaged viscoelastic constants of packaged samples. MRE experiments provide viscoelastic data as a function of position within samples and can be performed prior and post packaging, on samples including those with an optically opaque container or wrapper.

Keywords: Packaged food, Quality control, Non-invasive, MRI

---

*Corresponding author
Email address: `marco.gruwel@nrc-cnrc.gc.ca` (Marco L.H. Gruwel)

1. Introduction

Rheology plays a very important role in the modern food industry as it defines three major categories of food acceptability, appearance, flavor and touch. Evaluation of food texture, intermediate or final product quality control and shelf-life testing often involve rheological testing (Steffe, 1996). The food industry spends great efforts trying to control the extreme softening and textural degradation that occurs during food preservation, instantaneously or over time (Hiu, 2005; Taub & Sing, 1997; Kilkast, 2004). Many different techniques to measure viscoelastic properties of materials exist (Steffe, 1996). It is not the purpose of this paper to review all of these, however, it should be pointed out that most of these techniques are applied either in- or on-line on a production line or require access to the material without its packaging. Results from measurements performed this way are usually only valid for a narrow range of geometries, frequencies, etc.

The most common dynamic method used to measure viscoelastic properties of food stuffs is oscillatory testing (Steffe, 1996). Harmonic variation of stress or strain shows that viscoelastic properties are very sensitive to the chemical and physical composition of the materials. This makes the technique ideal to relate rheological properties to human sensory perception and to study the shelf-life of products (Rao & Skinner, 1986). Unfortunately, none of the techniques frequently used can be used on packaged, finished, products to test their quality during shelf-life. Recently, Magnetic Resonance Imaging (MRI) was used to monitor moisture distribution in multi-component food systems and spatially resolve its re-arrangement during storage (Ramos-Cabrer *et al.*, 2006). It was also shown, using the NMR MOUSE, that magnetic resonance presents a good option for non-invasive assessment of micro-structural parameters in manufacturing and in the supply chain (Haiduc *et al.*, 2007). Although MRI provides information on (micro) structural features such as size and spatial distribution by means of different water relaxation parameters of these structures, it does not provide direct information on physical properties such as shear.

Recently, Dynamic Mechanical Analysis (DMA) (Jones, 1999) was used to validate Magnetic Resonance Elastography (MRE) measurements of shear in agarose gels (Chen *et al.*, 2005). DMA analysis was performed on pre-formed disks of agar gel poured in petri dishes in order to control slab thickness. The experiments provided values of the shear modulus as a bulk parameter. Similar experiments have been performed using mechanical compression tests (Hamhaber *et al.*, 2003). MRE on the other hand is capable of providing data as a function of position within the sample. This is an extremely valuable asset as this allows the study of complete end products of a food processing unit, without the need to prepare samples for study. In many cases MRE measurements can be performed non-invasively, without having to remove the packaging, allowing for easy spatial mapping of viscoelastic properties, especially useful for products with complex compositions. MRE is a phase-contrast magnetic resonance imaging technique to map spatial displacement patterns corresponding to harmonic shear waves initiated by the mechanical oscillations of a specially designed actuator attached to the object (Lewa, 1992; Muthupillai *et al.*, 1995; Plewes *et al.*, 1995). Apart from many medical applications studying specific changes in tissue stiffness related to disease, *e.g.* liver fibrosis, cancer, *etc.* (Fatemi *et al.*, 2003), MRE has also been used to non-invasively study phase transitions in gels (Sack *et al.*, 2001).

We report the design and use of a simple but effective pneumatic actuator for the study of shear stress in food products and show its use in the determination of shear stress in pre-packaged fruit puddings as an example. MRE experiments enabled us to determine the shear modulus as a function of position in the samples and to monitor the distribution of fruit pieces. At present this technique is not useful for factory in-line quality control tests, however, it will be useful in the product development phase in the laboratory.

2. Materials and Methods

2.1. Magnetic Resonance

All MRE experiments were performed at room temperature using a 3T TrioTim medical MRI system Siemens, Germany). Samples were mounted on a sample holder (RF coil insert) equipped with rollers as shown in Figure 1. The roller axes were positioned parallel to the main magnetic field, to allow an oscillatory motion in the direction perpendicular to the field as shown in Figures 1 C and D. The sample holder was positioned in between two flexible, pneumatically driven actuators positioned on the side of the commercial RF head coil (Fig. 1B). Two speakers, delivering sound pressure through separate hard-walled flexible tubes, were used to drive the actuators in an out-of phase sense (180° phase shift). The direction of the main magnetic field B_0, the actuator-induced motion of the sample and the induced shear waves are shown in Figure 1 D. A programmable waveform generator, synchronized to the MRE pulse sequence, was used to deliver an acoustic frequency in the range of 20-150 Hz with actuator amplitudes up to 500 μm.

MRE experiments were performed with a modified Gradient Echo sequence using a 40° RF-flip angle, an echo time (TE) of 18 ms, a repetition time (TR) of 500 ms, a 10×10 cm^2 field of view (FOV), a 64×64 data matrix and sinusoidally shaped motion encoding gradients with strengths varying from 5 to 25 mT$\cdot$m^{-1}. Motion encoding, using the oscillating sinus-shaped gradients, was performed at 75-150 Hz, to match the oscillation frequency of the sample. The number of motion encoding gradient pairs, using one cycle per acquisition, was set to 8, *i.e.* 8 images were acquired at a different phase of the oscillation. Prior to motion encoding the amplitude of the acoustic signal was ramped over a period of 200 ms to avoid transient signals (Sack *et al.*, 2008).

The designed dual-actuator unit, shown in Figure 1B and C, can be easily mounted into a commercially available head coil (Siemens, 3T), by replacing the original head restrainers and adjusting the fit to the sample holder, providing good contact of the holder with the two actuators. It should be noted that, although the setup described in this work used a medical MRI scanner, the concept can easily be adapted to non-medical MRI equipment. An adaptation for micro-imaging of agar gels and frog eggs using a typical vertical bore magnet (56 mm, narrow bore, Oxford Instruments, Oxford, UK) using a home build piezo-electric actuator has been reported (Othman *et al.*, 2005).

Data processing was performed using MREwave, software obtained from Dr. Ehman's laboratory (Mayo Clinic, Rochester, MN). MREwave uses a local frequency estimation algorithm which provides an estimate of the local spatial frequency of shear wave propagation in the sample (Manduca *et al.*, 2001; Knutson *et al.*, 1994). The algorithm is relatively insensitive to phase noise and yields an accurate isotropic frequency estimation.

As an example of a packaged food product we used a small container of fruit pudding (98 g) containing water, sugar, fructose, coconut, citric acid, seaweed extract and a natural flavor (ABC Fruit Pudding, packaged for Loblaws Inc., Canada). The pudding was packaged in a hard plastic conical container with a bottom and top diameter of 5.5 and 6.7 cm, respectively, and a height of 3 cm. Coconut was added as small cubes with an approximate dimension of $1\times 1 \times 1$ cm^3.

2.2. Dynamic Compression

Dynamic compression tests were performed at ambient temperature on three samples using an Enduratec ElectroForce 3200 test instrument (Bose Corporation, MN, USA). Specimens of pudding without coconut inclusions, having a diameter of 18 mm and a height of 5 mm, were submitted to oscillating deformation in unconfined compression. The resulting forces were measured using a 500 g range load cell. To maintain a linear viscoelastic response, the oscillation amplitude was kept small (3% strain). The frequency was varied from 1 Hz to 20 Hz. Viscoelastic parameters were determined for each frequency from which the shear modulus was calculated, using a Poisson ratio of 0.49.

3. Statistics

Data in this study are represented as means $\pm$ standard deviation. Measurements were performed in triplicate. Data fitting was performed with QtiPlot (GPL) using the Marquardt-Levenberg algorithm.

4. Theory

In general, linear viscoelasticity of soft materials can be described by appropriate mechanical models composed of dashpots and springs (Steffe, 1996). Springs represent the solid element obeying Hooke's law while the dashpot introduces the Newtonian fluid characteristics. The two simple models combining one component of each are the Maxwell and the Voigt model (Catheline *et al.*, 2004). In the Maxwell model the elements are arranged in series, while in the Voigt model the components are connected in parallel. Both models provide a similar and good description of dispersion, however, the Voigt model was able to predict the frequency dependent shear attenuation much more accurately (Catheline *et al.*, 2004). Catheline *et al.* showed that the Voigt model describes agar gels and biological soft tissues best, especially in the frequency range of $f \geq 100$ Hz. At relatively high shear elasticity in the range of 5 kPa, the Voigt model provides an excellent approximation. However, when both elasticity and viscosity are relatively low, the Maxwell model does provide a good prediction of the speed of shear wave propagation, especially at lower frequencies (0-150 Hz).

Application of a sinusoidally modulated stress is known to result in a sinusoidally varying strain at the same frequency. This allows for the following definition of stress and strain:

$$\sigma = \sigma_0 \cdot exp(i\omega t) \tag{1}$$

$$\varepsilon = \varepsilon_0 \cdot exp(i(\omega t - \Delta\phi)) \tag{2}$$

Here σ represents stress while ε describes strain and $\Delta\phi$ the phase difference. The complex modulus describing their relation can thus be written as:

$$M(\omega) = \frac{\sigma_0}{\varepsilon_0} \cdot exp(i\Delta\phi) = M_1(\omega) + iM_2(\omega). \tag{3}$$

$M_1(\omega)$ is called the elastic (or storage) modulus, which is in phase with the applied oscillating strain, while $M_2(\omega)$ represents the viscous (or loss) modulus which is out of phase (90°) with the applied strain. For the Voigt model, these complex moduli are related to the elasticity modulus E, and the viscosity coefficient η, by:

$$M_1^V(\omega) = E \tag{4}$$

$$M_2^V(\omega) = \omega \cdot \eta \tag{5}$$

For the Maxwell model the moduli are defined as:

$$M_1^M(\omega) = \frac{E \cdot \omega^2\eta^2}{E^2 + \omega^2\eta^2} \tag{6}$$

$$M_2^M(\omega) = \frac{E^2 \cdot \omega\eta}{E^2 + \omega^2\eta^2} \tag{7}$$

Assuming we can describe the objects as isotropic homogeneous and incompressible systems, the propagation of shear waves can be modeled by the Helmholtz equation (Catheline *et al.*, 2004). The Helmholtz equation allows us to calculate the shear speed attenuation for the Voigt and

Maxwell model in terms of the Lamé coefficients μ_l and η_s for shear elasticity and viscosity, respectively, as:

$$c_s^V(\omega) = \sqrt{\frac{2(\mu_l^2 + \omega^2\eta_s^2)}{\rho(\mu_l + \sqrt{\mu_l^2 + \omega^2\eta_s^2})}}\,, \tag{8}$$

$$c_s^M(\omega) = \sqrt{\frac{2\mu_l}{\rho\left(1 + \sqrt{1 + \frac{\mu_l^2}{\omega^2\eta_s^2}}\right)}} \tag{9}$$

Usually, for biological tissues and gels, the density, ρ, is assumed to be 1000 kg$\cdot$m^{-3} as a very good approximation. For a pure elastic medium ($\eta = 0$) and according to the Voigt model, the speed of the shear waves becomes frequency independent. This can be considered the low-viscosity approximation in which $c_s^V(\omega) \approx \sqrt{\mu_l \cdot \rho^{-1}}$. In the limit of low viscosity, the Maxwell model provides $c_s^M(\omega) \approx \sqrt{2\mu_l \cdot \rho^{-1} \cdot \omega\eta_s}$ which indicates a frequency dependence. For viscoelastic media the shear wave speed is predicted to increase monotonically with frequency for either model outside the low viscosity limit.

5. Results and discussion

Figure 2 shows a scout image of the fruit pudding. The scout echo was obtained with a Fast Spin Echo sequence in order to obtain the contrast between the pudding and the coconut chunks. The bottom of the container is shown on the right hand side of the image where the pieces of coconut are indicated with arrows. Other slice orientations, not including pieces of coconut, could also be selected. However, for the purpose of showing the capabilities of the MRE technique and the data processing, we opted for an orientation containing a few stiff objects.

The exact slice orientation as used for the scout image in Figure 2 was applied in the MRE experiments. MRE was performed at four different actuator frequencies; 75, 100, 125 and 150 Hz, to study the frequency dependence of the shear modulus. A typical data set for the 100 Hz actuator frequency is shown in Figure 3. The oscillatory motion from the actuator was applied perpendicular to the dotted line in Figure 3A in a top-bottom fashion for convenience, as shown in Figure 1D with respect to the external magnetic field B_0. This makes the shear wave propagate horizontally from right to left in all the images shown. Knowing the pixel resolution in the MR images, the wavelength of the shear waves could be calculated from phase images, shown in Figure 3A,B. The speed of the transverse waves could thus be obtained at each frequency. Figure 4A shows the slight frequency dependence of the wave propagation speed, indicating that the puddings are not a pure elastic medium. For viscoelastic media such as biological tissue and gels, the shear wave speed increases monotonically with the frequency, ω, due to dispersive coupling with viscosity. The higher the slope in Figure 4A, the more viscous the material. This relation can be used to check the shelf-life, for instance, of food products against changes in viscosity without having to remove the materials from its wrapping or container.

To calculate the shear modulus, μ_l, for the fruit pudding as a function of position in the sample, a Local Frequency Estimation (LFE) algorithm was used (Manduca *et al.*, 2001). LFE is a robust algorithm that yields accurate and isotropic estimates for the local frequency. For the area in between the two coconut pieces (see Figure 3D), an averaged local frequency estimate of f_{LFE} = 96.2±6.5 Hz which is a very good approximation of the actuator frequency of 100 Hz. The LFE algorithm is relatively insensitive to noise, making it a perfect tool in combination with MR which sometimes can suffer from low signal to noise ratios. The LFE algorithm has limited resolution, causing blurring of the frequency estimate near sharp boundaries. As a result the estimation of the shear modulus suffers from errors at the edge of sample and, for the same reason, near inclusions when the local stiffness changes rapidly. However, if the actual value of the shear modulus of inclusions is not of interest, the LFE is an excellent algorithm to detect these inclusions as they will be detectable as a change in local frequency (see Figure 3D). Using the LFE algorithm thus allows for the accurate spatial detection of inclusions, however, not for the determination of their stiffness (in most cases, depending on the frequency used). Another algorithm, AIDE, based on algebraic inversion of the equations of motion (Helmholtz equation), requires the calculation of second derivatives which makes this algorithm very sensitive to noise and not so suitable for MR. In Figure 3C a map of the calculated shear modulus is shown. The area in between the inclusions is characterized by a shear modulus, μ_l =0.75±0.15 kPa. This value compares well with previously reported shear moduli for alginate gels (LeRoux *et al.*, 1999). Seaweed (alginate) is an important component of the fruit pudding. It should be mentioned that the shear and viscous properties of alginate gels strongly depend on the amount of cross-linking which is controlled by very small amounts of bi-valent cations. For the measured $c_s(\omega) < 1$ m·s^{-1} in the excitation frequency range of $75 \leq f \leq$ 150 Hz, we observe the Voigt model to provide a good description of the visco-elastic properties of the material. According to eqn.8, using a two parameter fit for viscosity and the shear modulus, the viscosity of the fruit pudding measured at 100 Hz is approximately 0.49±0.03 Pa·s (see Figure 4A). The same fit resulted in a value of 0.61±0.02 kPa for the shear modulus at 100 Hz. The density of the fruit pudding was kept fixed at 1000 $kg \cdot m^{-3}$ throughout the data fitting. The observed frequency dependence of the shear wave velocity shown in figure 4A could not be fitted to the Maxwell model as described by eqn. 9.

Using dynamic compression, a separate measurement of the shear modulus in samples of the fruit pudding was performed in parallel. The relative softness of the material prevented measurements above 20 Hz. Figure 4B shows the obtained frequency dependence. This data was fitted to a linear relationship between shear stress and frequency in order to extrapolate the measurements to 100 Hz. The obtained fit predicted a shear modulus of 0.69 kPa (see Fig. 4B), a value that corresponds well with that obtained from MR elastography measurements. The frequency dependence of the shear modulus in the fruit pudding (Fig. 4B) is small in the frequency range of 1-100 Hz. A Maxwell model would predict a much larger frequency dependence in this range. Together with the MRE results, the dynamic compression measurements indicate that the Voigt model provides the best description of the visco-elastic properties of these fruit puddings.

In conclusion, we have shown that MRE can be used to non-invasively determine the spatial distribution of viscoelastic properties from food stuffs. MRE experiments could be a helpful addition to the development of multi-component food products and could be used for highly automated quality control checks in the laboratory. Although a medical 3T scanner was used in the experiments described above, these experiments can also be performed at standard laboratory MR systems, including microimagers (Othman *et al.*, 2005), for samples of different shape and size, depending on the magnet bore width. Of course, with a decrease in sample size, an increase in oscillatory frequency is needed. This can be accommodated switching to piezo-electrical or electro-mechanical actuators. The use of MRE also allowed for an extension of the dynamic range of frequency measurements. Dynamic compression measurements could only be performed up to 20 Hz due to the softness of the material, however, using MRE we were able to measure the shear modulus up to 150 Hz. The relation $c_s = \lambda \frac{\omega}{2\pi}$ and the field of view (FOV) of the MR image set a lower excitation frequency limit for the experiments while an upper limit is essentially set by the strength of the used encoding gradients.

Acknowledgements

The authors thank Dr. Richard Ehman for introducing them to MRE using pneumatic actuators and Dr. Chris Bowman for helpful discussions. Drs. Valérie Pazos and Patricia Debergue are thanked for their help with the dynamic compression experiments.

References

Catheline, S.; Gennisson, J. L.; Delon, G.; Fink, M.; Sinkus, R.; Abouelkaram, S.; Culioli, J. (2004). Measuring of viscoelastic properties of homogeneous soft solid using transient elastography: an inverse problem approach. *Journal of the Acoustic Society of America, 116*, 37343741.

Chen, Q.; Ringleb, S. I.; Hulshizer, T.; An, K.-N.(2005). Identification of the testing parameters in high frequency dynamic shear measurement on agarose gels. *Journal of Biomechanics, 38*, 959963.

Fatemi, M.; Manduca, A.; Greenleaf, J. F. (2003). Imaging elastic properties of biological tissues by low-frequency harmonic vibration. *Proceedings IEEE 91*, 15031519.

Haiduca A.M.; Trezza E.E.; van Dusschoten D.; Reszka A.A.; and van Duynhoven J.P.M. (2007). Non-invasive 'through-package' assessment of the microstructural quality of a model food emulsion by the NMR MOUSE *Food Sci. Tech., 40*, 737-743.

Hamhaber, U.; Grieshaber, F. A.; Nagel, J. H.; Klose, U. (2003). Comparison of quantitative shear wave MR-elastography with mechanical compression tests. *Magnetic Resonesonance in Medicine, 49*, 7177.

Hiu, Y., Ed. (2005). *Handbook of food science, technology and engineering, Vol. 1* Marcel Dekker Inc., New York, NY, USA.

Jones, D. (1999).Dynamic analysis of polymeric systens of pharmaceutical and biomechanical significance. *International Journal of Pharmaceuticals, 179*, 167178.

Kilkast, D., Ed. (2004). *Texture in food. Volume 2: Solid foods*; Woodhead Publishing Ltd., Cambridge, UK.

Knutsson, H.; Westin, C. F.; Granlund, G. (1994). Local multiscale frequency and bandwidth estimation. *Proceedings ICIP-94. IEEE International Conference Image Processing*, pp. 3640.

LeRoux, M. A.; Guilak, F.; Setton, L. A. (1999). Compressive and shear properties of alginate gel: effects of sodium ions and alginate concentration. *Journal of Biomedical Material Reseach, 47*, 4653.

Lewa C.J. (1992). MRI response in the presence of mechanical waves, NMR frequency modulation, mechanical waves as NMR factor. *Acustica, 77*, 43-45.

Manduca, A.; Oliphant, T. E.; Dresner, M. A.; Mahowald, J. L.; Kruse, S. A.; Amromin, E.; Felmlee, J. P.; Greenleaf, J. F.; Ehman, R. L.(2001). Magnetic resonance elastography: non-invasive mapping of tissue elasticity. *Medical Image Analysis, 5*, 237254.

Muthupillai, R.; Lomas, D. J.; Rossman, P. J.; Greenleaf, J. F.; Manduca, A.; Ehman, R. L. (1995). Magnetic resonance elastography by direct visualization of propagating acoustic strain waves. *Science, 269*, 18541857.

Othman S.F.; Xu H.; Royston T.J. and Magin R.L. (2005). Microscopic magnetic resonance elastography (μMRE). *Magn. Reson. Med., 54*, 605-615.

Plewes, D. B.; Betty, I.; Urchuk, S. N.; Soutar, I. (1995). Visualizing tissue compliance with MR imaging. *Journal of Magnetic Resononance Imaging ,* *5*, 733738.

Ramos-Cabrer, P.; van Duynhoven, P.M.; Timmer, H. and Nicolay K. (2006). Monitoring of moisture redistribution in multicomponent food systems by use of magnetic resonance imaging. *J. Agric. Food Chem., 54*, 672-677.

Rao, V.; Skinner, G. (1996). *Engineering properties of foods*; Marcel Dekker Inc., New York, NY, USA, pp. 215254.

Sack, I.; Beierbach, B.; Hamhaber, U.; Klatt, D.; Braun, J. (2008). Non-invasive measurement of brain viscoelasticity using magnetic resonance elastography. *NMR in Biomedicine, 21*, 265271.

Sack, I.; Buntkowsky, G.; Bernarding, J.; Braun, J. (2001). Magnetic resonance elastography: a method for the noninvasive and spatially resolved observation of phase transitions in gels. *Journal of the American Chemical Society, 123*, 1108711088.

Steffe J. (1996) *Rheological methods in food process engineering, 2nd Edn.*; Freeman Press, East Lansing, MI, USA.

Taub, I.; Singh, R. (1997). *Food storage stability*; CRC-Press, Boca Raton, FL, USA.

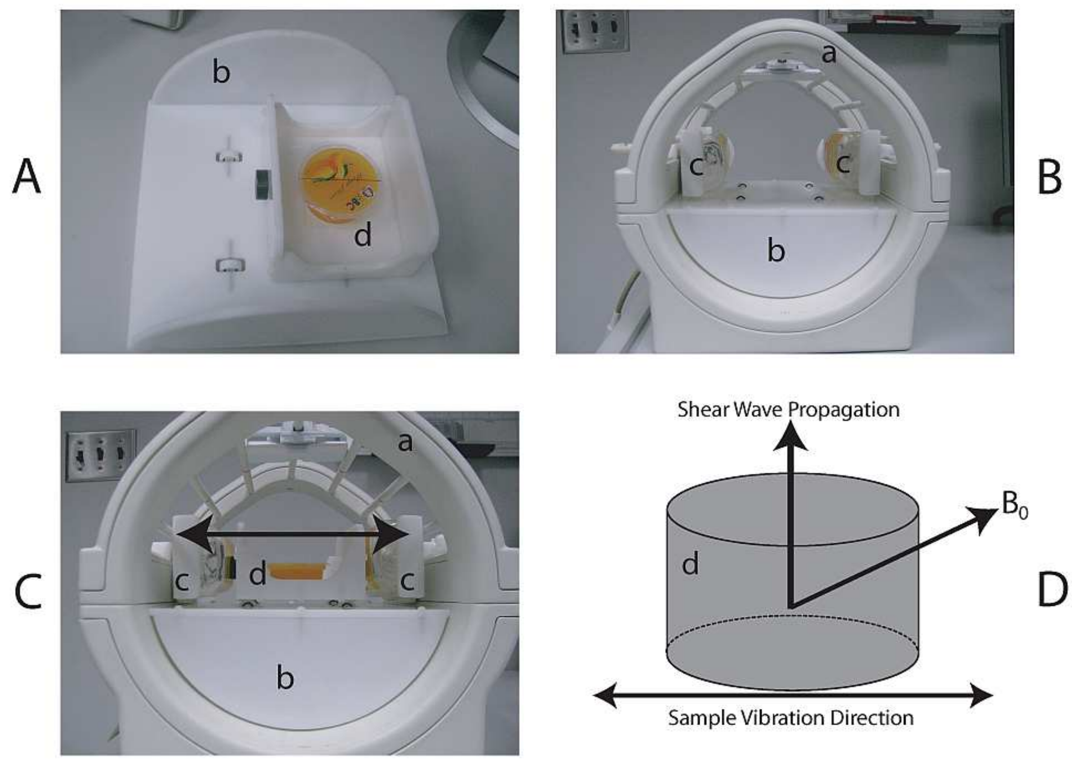

Figure 1: The pneumatic dual actuator set up. A) Removable sample holder with sample(d) shown on top of the coil-insert(b) with rollers to accommodate a left-right motion caused by the actuators. B) Position of the actuators(c) with respect to the coil. C) Complete set up of coil(a), coil-insert(b), actuators(c) and sample bed with sample(d) in the commercial head coil. D) Motion is induced by the actuators(c) from left to right in Fig. C, the orientation of the main magnetic field B_0 is indicated in Fig. D with respect to the orientation of the shear waves and the actuator motion.

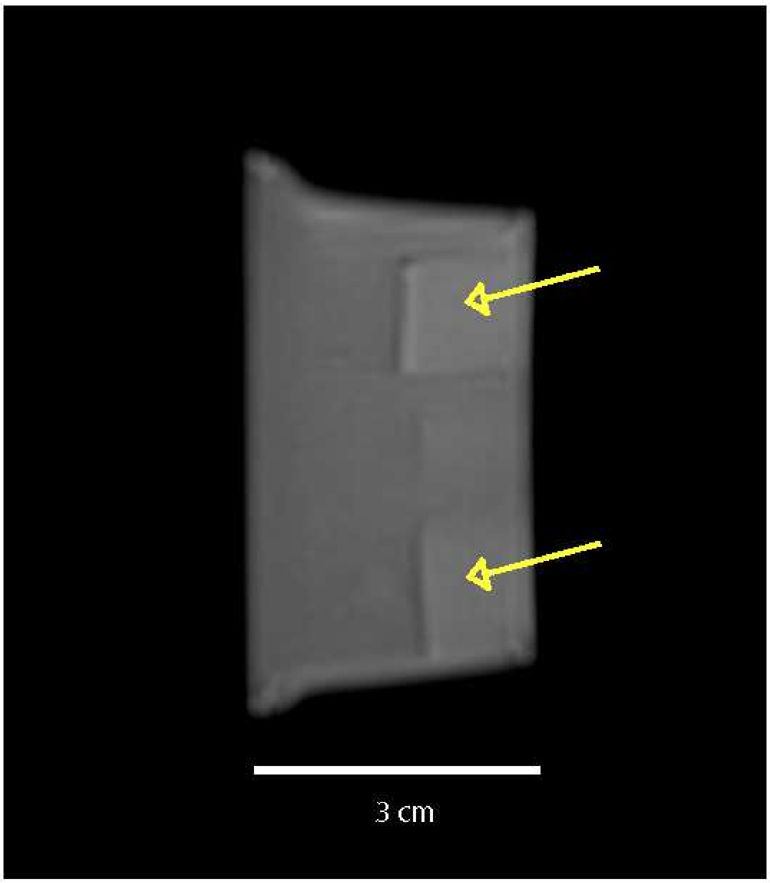

Figure 2: An MRI scout image clearly showing the chunks of coconut as indicated by the arrows. This slice orientation (5mm thick) was used for the MRE experiments.

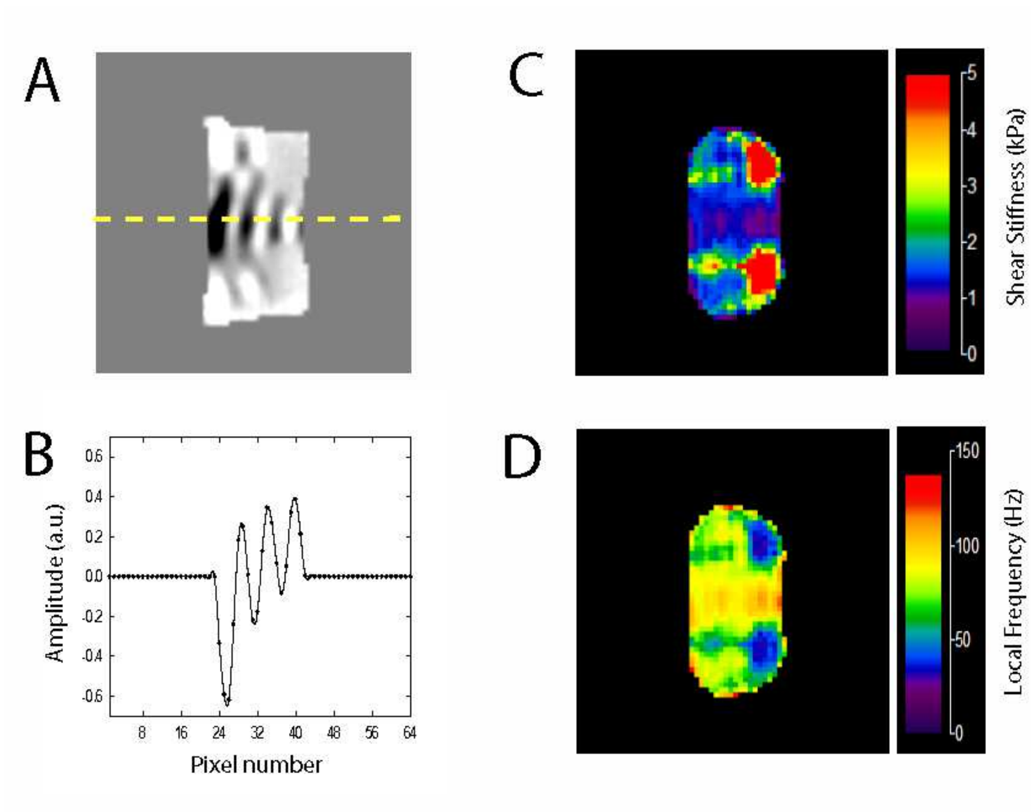

Figure 3: A) Wave image obtained at 100 Hz of mechanical oscillation. In the locations of the coconut pieces, the shear waves were strongly attenuated. Wave propagation through the center of the sample can clearly been seen. B) Amplitude oscillations obtained at the dotted line from the phase image in A. C) The estimated shear stiffness, using the Local Frequency Estimation algorithm. The coconut pieces can now clearly be distinguished due to their different composition from the rest of the pudding. Note that the shear modulus between the two stiffer coconut inclusions appear rather homogeneous. D) The local frequency as calculated by the LFE algorithm as a function of position. As in C for the shear modulus, the local frequency is well defined in the area between the coconut inclusions.

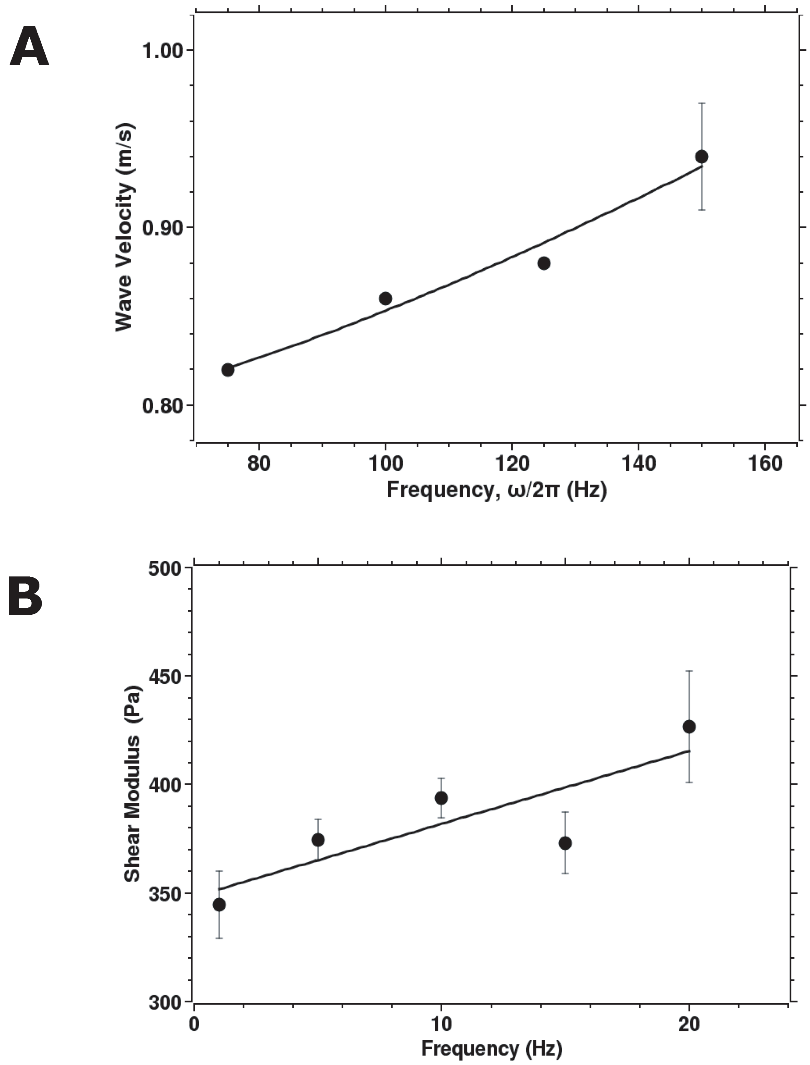

Figure 4: A) Frequency dependence of the shear wave velocity in fruit pudding. The solid curve represents a fit of the data to eqn. 8, using μ_l= 0.61±0.02 kPa and η_s= 0.49±0.03 Pa·s. The density of the pudding was fixed at 1000 kg·m^{-3}. B) Frequency dependence of the shear modulus, measured by dynamic compression. The shear modulus was fitted to a linear frequency dependence; $\mu_l(\frac{\omega}{2\pi})$= (348±15) + (3.4±1.2)$\frac{\omega}{2\pi}$.